RESEARCH ARTICLE

BioDiscovery

OPEN ACCESS

NRF2 inhibition causes repression of ATM and ATR expression leading to aberrant DNA Damage Response

Hilal S. Khalil, Yusuf Deeni*

School of Science, Engineering and Technology, Abertay University, Dundee, DD1 1HG, United Kingdom

Abstract

Nuclear factor (erythroid-derived 2)-like 2 (NRF2) is a master regulator of the antioxidant response (AR) pathway and functions as a transcription factor for basal and oxidative stress-induced expression of a battery of detoxification enzymes and cytoprotective genes. Recent evidence has also demonstrated a role of NRF2 in driving resistance of numerous cancers to chemotherapeutic agents. ATM and ATR are serine/threonine kinases that are activated following DNA damage and function as central components of DNA Damage Response (DDR) pathway. Activities of these kinases cause cell cycle arrest and activate DNA repair signals leading to cytoprotection against genotoxic agents. In this study, we elucidated the roles of ATM- and ATR- dependent DDR and NRF2- mediated AR pathways in promoting cytoprotection following cisplatin challenge in ovarian cancer cell line models. We also determined whether these pathways were inter-dependent for full activation following genotoxic insults and as such demonstrated crosstalk in their signaling mechanism to elicit cytoprotective pathways. Treatment with cisplatin caused NRF2 induction and generation of reactive oxygen species (ROS) that caused cytotoxicity in ovarian cancer cells. This was attenuated by the ROS scavenger N-Acetyl cysteine, implicating NRF2 function in cytoprotection against cisplatin. Treatment with retinoic acid (RA) caused down regulation of NRF2, disruption of AR pathway, significant accumulation of ROS and enhanced cisplatin cytotoxicity. Interestingly, RA treatment also led to repression of total ATM and ATR proteins and aberrant DDR activation following cisplatin challenge. In order to determine whether the RA induced ATM and ATR repression was dependent on NRF2 inhibition, we silenced NRF2 using SiRNA. This caused transcriptional repression of both *ATM* and *ATR* expression as determined by their promoter driven luciferase assays. Thus, NRF2 inhibition led to DDR suppression by down-regulating ATM and ATR that led to enhanced cytotoxicity. These findings demonstrate mechanism of crosstalk between the AR and the DDR pathways and extend the scope of NRF2 in promoting cancer therapeutic resistance.

Citation: Khalil HS, Deeni Y. NRF2 inhibition causes repression of ATM and ATR expression leading to aberrant DNA Damage Response. *Biodiscovery* 2015; **15**: 1; DOI: 10.7750/BioDiscovery.2015.15.1

Received: 18 January 2015; **Accepted:** 26 March 2015; **Available online/Published:** 28 March 2015

Keywords: NRF2, DNA-damage, ATM, ATR, antioxidant pathway

*Corresponding Author: Y. Deeni, email: y.deeni@abertay.ac.uk

Conflict of Interests: None declared.

Introduction

Nuclear factor (erythroid-derived 2)-like 2 (NRF2) is a leucine zipper transcription factor encoded by the *NRF2* gene that is located on the long arm of human chromosome 2 [1]. It is the master regulator of the antioxidant response (AR) pathway for driving both basal and oxidative stress-induced transcription of a battery of detoxification enzymes and cytoprotective genes [2] as well as other signal transduction pathways [1]. This is achieved by heterodimerisation of NRF2 with small MAF proteins and binding to some *cis*-acting factors called Antioxidant Response Elements (AREs) or electrophile response elements (EpREs) within the promoters of these genes [3, 4]. Under basal conditions, little free NRF2 is available in the cytoplasm and for translocation to the nucleus to drive the basal transcription of target genes. Most of the remaining cytosolic NRF2 is held by KEAP1, a cytoplasmic NRF2-binding adaptor and electrophiles sensor protein, which tethers NRF2 for association with the Cul3-based E3 ubiquitin ligase to promote its degradation by the 26S proteasome [5]. Under oxidative stress or in the presence of NRF2 inducers or activators, a number of cysteine residues of KEAP1 become oxidised to cause

conformational changes in the KEAP1 structure. This allows NRF2 to escape from being targeted by the 26S proteasomal degradation machinery and to accumulate in the nucleus to further induce the transactivation of ARE-containing genes in order to restore redox homeostasis [6].

NRF2 is a recognised player in cellular proliferation and adaptation to reactive oxygen species and in driving resistance of numerous cancers to chemotherapeutic agents [7]. Importantly, NRF2 activation and KEAP1 inactivation mutations leading to permanent constitutive adaptive activation of the NRF2 pathway are increasingly observed in cancers [8, 9, 10] and other diseases [11, 12]. It is well known that several therapeutic strategies, for example anticancer radiotherapy and chemotherapy, largely depend on ROS manipulation to induce cytotoxicity. More recently, there is a growing body of evidence implicating NRF2 and ROS in the promotion of cellular proliferation and therapeutic resistance in cancer cells [13-17].

Exposure of proliferating cells to physical, chemical or biological genotoxic stresses activates a cascade of signalling events termed as the DNA Damage Response (DDR). The DDR preserves genetic stability by detecting DNA lesions, activating cell cycle checkpoints and promoting DNA damage repair [18-21]. The common denominator integrating these forms of genotoxic stresses and eliciting the signalling cascade is increased production of ROS as harbinger to DNA damage [22-27]. Chemical agents such as drugs used in cancer chemotherapy are also able to induce some form of DNA lesions [28]. While chemotherapy drugs which function as alkylating agents, such as methyl methane sulfonate (MMS) and temozolomide, attach alkyl groups to DNA bases, other drugs such as cisplatin and psoralen, introduce covalent links between bases of the same or different DNA strands [29]. These insults trigger the DDR pathway, which is primarily umpired by proteins of the phosphatidylinositol 3-kinase-like protein kinase (PI3KKs) family: Ataxia telangiectasia mutated (ATM), Ataxia telangiectasia and Rad3 related (ATR) and DNA dependent protein kinase (DNA-PK). These are constitutively transcribed proteins, which rapidly undergo posttranslational activation following DNA damage and replication errors [28, 30, 31]. Once activated, the ATM and ATR protein kinases phosphorylate and in turn activate their downstream substrates P53, checkpoint kinases (CHK1, CHK2) and H2AX [32-34]. Checkpoint proteins arrest the cell cycle transiently, P53 activation links the repair responses with cell cycle progression and apoptotic pathway, while H2AX focus formation at the DNA lesion recruits important repair enzymes at the damaged site [35-37]. Checkpoint arrest could also activate enzymes involved in apoptosis, permanently leading to cell senescence or cell death [32]. The fate of cell depends on the pathway activated, which is decided by the extent of DNA damage. [38, 39]. Thus DDR is a signal transduction pathway that is coordinated to accord with other cellular activities such as cell cycle progression and programmed death. Activated ATR/ATM-regulated DNA damage response pathway is observed in tumour cells during early cancer cell progression and constrains tumour progression. High levels of marker enzymes such as phosphorylated kinases, ATM and CHK2, and phosphorylated histone H2AX and P53 which are implicated in different DNA damage repair pathways have been observed in early superficial lesions and early invasive tumours, with low levels observed in more advanced stages of urinary bladder [40].

Ovarian cancer cells have been shown to evolve intricate mechanisms of cellular resistance towards both ROS and DNA damaging agents as demonstrated by a very robust antioxidant sensing and ROS neutralising mechanisms as well as a highly efficient DNA repair system [7, 41-44]. ROS can trigger DNA damage which elicits ATM- and/or ATR-dependent signalling pathways to control cell cycle progression, apoptosis, and DNA repair, however how ATM and ATR are transcriptionally controlled and then activated following ROS insults is not fully understood. Although ATM deficiency is associated with elevated cellular ROS, there is no evidence of a direct integration node and a crosstalk between the cellular ATM/ATR-dependent responses with NRF2-centred adaptive system that regulates cellular ROS.

This study aims to investigate and identify direct crosstalk between the NRF2 antioxidant response (AR) pathway and ATM/ATR dependent DDR pathways following genotoxic insults in order to determine their potential interdependence to elicit repair responses and signalling contribution culminating in cytoprotection. By utilising transcriptional reporter assays, DDR and AR inhibition strategies and analysing functional activation of AR and DDR pathways following dose and time dependent genotoxic insults, we have identified a node of functional integration of the two pathways. We have demonstrated that inhibition of AR leads to inefficient activation of DDR and that this is as a consequence of transcriptional repression of both *ATM* and *ATR* genes. Thus, this study reveals a new mechanism of crosstalk between AR and DDR pathways and as such opens up novel avenues of targeting DDR and sensitisation of resistant ovarian cancer cells by way of manipulating the AR pathway.

Materials and Methods

Cell lines, culture conditions and treatments

Human ovarian cancer cell lines PEO1 and SKOV3 were maintained in RPMI media (Gibco® Invitrogen, UK) supplemented with 10% foetal bovine serum (FBS),

2 mM glutamine, 1 mM sodium pyruvate, 100 µg/ml streptomycin and 100U/ml penicillin in an atmosphere of 5% CO_2. For Retinoic acid (RA) treatments, a stock solution of 40mM was made in 100% ethanol in amber eppendorf tubes pre-aired with nitrogen gas. Once the stock solution was made, it was bubbled again with nitrogen gas and closed, stored at -80°C protected from light until further use. A final concentration of 2.5µM was used for treatments. For reducing conditions, 100mM N-Acetyl Cysteine (Sigma-Aldrich) was prepared in deionised water and diluted to a final concentration of 10mM with media during treatments. Specific ATM kinase inhibitor, KU60019 (Selleckchem, UK) was used at a final concentration of 10µM. A freshly prepared Cisplatin (Sigma-Aldrich) solution was made with PBS in amber tubes and used within 24 hours (h) by diluting to the required concentrations. 2′,7′-Dichlorofluorescin diacetate (Sigma-aldrich) solution was made with Dimethylsulfoxide in amber tubes to a concentration of 50mM and stored at -20°C in dark. For cytotoxicity assay, 3-(4,5-Dimethylthiazol-2-yl)-2,5-Diphenyltetrazolium Bromide (MTT) was used by making a stock solution of 5mg/mL in PBS and filter sterilising it. The solution was stored at 4°C in dark until used.

Reactive Oxygen Species (ROS) detection

ROS detection assay was performed by using 2′,7′-Dichlorofluorescin diacetate (DCFDA) staining (Sigma-Aldrich). Briefly, cells were seeded at a density of 0.2×10^5 cells/well of opaque flat bottom 96-well tissue culture plates in 100µl media without phenol red and allowed to grow for 18h. On the day of treatment, wells were washed with pre-warmed PBS and 100µL of phenol red-free media having the drugs at desired concentrations were added to the required wells. Towards the end of treatment period, stock solution of DCFDA was added to each well containing 100µL pre-existing media to achieve a final concentration of 25µM and incubated for 45 minutes (min) at 37°C. Fluorescence signal intensities indicating ROS levels were recorded by taking readings using 96-well fluorescent multi plate reader (MODULUS™, Promega) using excitation and emission spectra of 485nm/535nm.

Protein extraction and immunoblotting

For immunoblotting, cells were seeded in 60mm tissue culture plates and grown until 70% confluent. At the time of protein harvest, cells were trypsinized (Gibco® Invitrogen) and washed with PBS. Protein lysates were prepared using RIPA buffer (Pierce Biotech) supplemented with protease and phosphatase inhibitor cocktail (Pierce Biotech) and subjected to sonication of 2 cycles for 10 seconds at 50% pulse. The final mixture was shaken gently on ice for 15 min and the protein supernatant was obtained by centrifuging the lysates at 14000 g for 15 min. Proteins obtained were quantified by Bradford assay (Sigma-Aldrich) using BSA as a standard and sample buffer (Nupage LDS, Invitrogen) was added to protein lysates, heated at 70°C for 20 min and stored at -20°C until further use. Once the protein lysates prepared, they were loaded into wells of 4-12% gradient SDS-polyacrylamide gels (Nupage® Bis-Tris gels, Life Technologies) and subjected to electrophoresis at 200 Volts for 1-2h. Following this, proteins were transferred to polyvinylidene difluoride membranes (GE Amersham) using the XCell SureLock Mini-Cell system (Invitrogen) at 50 Volts for 90 min and processed using a commercially available kit (WesternBreeze™ Chromogenic Immunodetection Kit, Invitrogen). Non-specific reactivity was blocked by incubation with the blocking reagent supplied in the kit. Membranes were further treated by incubating with primary antibodies (Table 1) for 2 hours at room temperature or overnight at 4°C, followed by incubation for 30 min at room temperature with appropriate secondary anti mouse or anti rabbit antibody supplied in the kit. Bands were visualized with the BCIP/NBT based chromogenic substrate. For loading control, immunoblotting of the same lysates was performed using b-Actin antibody (Abcam Bioscience, UK).

Table 1. Antibodies used in the study.

Antibody	Host	Catalogue Number	Company
NRF2	Rabbit	Sc-722	Santa Cruz
Phospho NRF2 S-15	Rabbit	ab76026	Abcam
ATM	Rabbit	ab32420	Abcam
ATR	Rabbit	ab10312	Abcam
Phospho ATM S-1981	Mouse	ab36810	Abcam
Phospho ATR S-426	Rabbit	2853	CST
P53	Rabbit	2527	CST
Phospho P53	Mouse	9286	CST
Phospho Chk2	Rabbit	2197	CST
γ-H2AX	Rabbit	9718	CST
b-Actin	Rabbit	1801	Abcam
Alexa fluor 488 conjugated secondary antibody	Rabbit	ab150077	Abcam
Alexa fluor 568 conjugated secondary antibody	Rabbit	ab175471	Abcam
Alexa fluor 568 conjugated secondary antibody	Mouse	ab175473	Abcam
Alexa fluor 488 conjugated Secondary antibody	Mouse	ab150117	Abcam

Proliferation and cytotoxicity assays

Proliferation and cytotoxicity assays were performed using 3-(4,5-Dimethylthiazol-2-yl)-2,5-Diphenyltetrazolium Bromide (MTT). Briefly, cells were seeded at a density of 0.5×10^4 cells in triplicates in complete media per well in 96-well plate and allowed to attach for 18h. On the day of treatments, old media was removed and 80µL of media containing drugs at the desired concentrations were added and the plate incubated for the required period of time. On the day of assay, 20µL of the 5mg/mL MTT stock was added to each well and plate further incubated for 4h. Following this, the old media with MTT was removed, cells gently washed with pre-warmed PBS and 100µL of DMSO added to solubilise the internalised MTT by shaking over an orbital shaker for 15 min. Absorbance of the released dye was measured and recorded using multiplate reader (MODULUS™, Promega) at 540nm.

Luciferase reporter assays and cell transfection

For the analysis of promoter activities and transcriptional regulation, the promoter regions of ATM and ATR genes were cloned in PGL3 basic vector (Promega) to generate promoter driven luciferase expression system for utilisation in Dual Luciferase Reporter assays (Promega) as described in [30]. Briefly, cells were seeded in 24 well plates at a density of 2×10^5 cells per well and allowed to attach for 18h. Following this, cells were either transfected with 1µg of empty PGL3 basic vector (Promega) or PGL3 basic vector with 1kb cloned fragments of ATM or ATR promoters driving the expression of luciferease gene using Lipofectamine 3000® as transfection reagent according to manufacturer's instructions (Life technologies). Co-transfection was also performed with 0.2µg of pRL-CMV vector (Promega) to provide for an internal control of transfection. Following this, cells were allowed to grow for 24h, subjected to desired treatments, lysed and protein lysates transferred to opaque white bottom 96-well plates. The dual luciferase activity of fire fly luciferase (from cloned promoters) and Renilla (internal control) in the harvested lysates was measured sequentially by following manufacturer's instructions (Promega) and taking luminescence readings in luminometer (MODULUS™, Promega). To determine NRF2 dependent transcriptional antioxidant response following different treatments, stable clones of MCF7 cells carrying PGL3 vector with a cloned 8 copies of *Cis*-Antioxidant Response Elements (ARE) reporter construct (AREc32) was used [45]. Briefly, AREc32 was seeded in 96 well plates at a density of 1.5×10^4 cells per well and allowed to attach for 18h. Next day, cells were washed with pre-warmed PBS and 100µL of media containing the required treatments was added and further allowed to incubate for the desired time period. Towards the end of treatment, 100µL of the reconstituted luciferase reagent (Bright Glo Luciferase, Promega) was added in each well containing 100µL of pre-existing media and plate incubated at 37°C for 10 min. 80µL of the cell lysate was transferred to opaque white bottom 96-well plate for luminescence detection in luminometer (MODULUS™, Promega) while the remaining 20µL was subjected to Bradford assay to estimate protein content for the normalisation of luminescence signal. To determine the transcriptional activity of NRF2 in PEO1 and PEO4 cell lines, basic PGL3 vector (Promega) containing cloned ARE promoter elements was transfected into the cell lines and subjected to Dual Luciferase reporter assay (Promega) as described earlier.

SiRNA transfection

Small inhibitory RNA (SiRNA) was used to knockdown NRF2 (Qiagen). For SiRNA transfection, cells were either seeded in 24 well plates (0.5×10^5 cells), or 60mm plates (0.5×10^6 cells) and allowed to grow for 18h. Following this, cells were either co-transfected using 20pmol SiRNA and 1µg of different PGL3 promoter constructs (24 well plate) or 75pmol and 100pmol SiRNA only (60mm plate) and incubated for further 24h. Cells transfected in 24 well plate were further processed for Dual luciferase assay as described earlier while those in 60mm plate was subjected to immunoblotting analysis. In all cases, transfection was performed using Lipofectamine 3000 (Life technologies) according to manufacturers instructions.

Enzyme Linked Immunosorbent Assay (ELISA)

ELISA was performed by seeding exponentially growing cells in triplicates at a density of 1.5×10^4 cells in complete media in opaque 96-well flat bottom plates and allowed to attach for 18h. The next day, following relevant treatments, cells were washed three times with ice cold PBS, fixed in 3.5% paraformaldehyde in a standard PBS at room temperature for 30 min. Following this, cells were gently washed twice with 1 ml of PBS, permeabilized with 0.1% triton X-100 in PBS for 10min, and following three washed with PBS, blocked with 1% goat serum, 1% bovine serum albumin in PBS containing 0.05% Triton X-100 for 30 min. Cells were then incubated with relevant primary antibody (Table 1) diluted in blocking solution overnight, washed three times with 0.1% Triton X-100 in PBS for 5 min, and then incubated with either Alexa Fluor 488 or 568 conjugated goat anti-rabbit or anti mouse antibodies (Abcam) for 1h. After subsequent washing three times with the 0.1% Triton X-100 in PBS for 5 min, cover slips with cells were mounted on slide using 4',6-Diamidino-2-Phenylindole, Dihydrochloride (DAPI)-containing mounting reagent (Vectashield, Vector Laboratories). Fluorescence signal intensities were quantified by taking readings using relevant channels in multiplate fluorimeter (MODULUS™, Promega). To normalise ELISA data of fluorescence signal, cells in the same wells were stained

with coomassie brilliant blue stain (SIGMA) for 1h, washed and 10% SDS solution was added to release the absorbed dye for 10min while shaking. The absorbance values at 595nm were then recorded using multiplate absorbance reader (MODULUS™, Promega) and data used to normalise the fluorescence values of ELISA.

Statistical analysis

All statistical analysis were performed using statistical software SPSS (IBM, version 22). Test for normality of data was determined by Shapiro-Wilk and Kolmogorov and Smirnov tests. The significance (p value) of differences of pooled results was determined by either independent t tests or One WAY ANOVA followed by post hoc Tukey's tests. Significance was defined as * = $p< 0.05$, ** = $p<0.01$, *** = $p<0.001$. Quantitative analysis of raw immunoblots was performed by capturing the immunoblot images in high resolution TIFF format files using a charge-coupled-device camera (AxioCam MRc, Carl Zeiss). Data were generally expressed as mean ± S.D for individual sets of experiments.

Results

Cisplatin induced cytotoxicity is partially relieved by neutralising Reactive Oxygen Species (ROS)

Ovarian cancer cells have been documented to show different degrees of resistance to cisplatin, which is the main contributing factor for the development of drug resistance in this type of cancer [46]. This has been attributed to both enhancement of DNA repair efficiencies [47] and cellular antioxidant potential [48]. Firstly, in order to identify differences in cisplatin resistance in cell line models used here, we exposed PEO1 and PEO4 ovarian cancer cell lines to varying concentrations of cisplatin for 24h. Consistent with previous reports [49], we found that PEO4 was more resistant to cisplatin treatment at all the concentrations of the drug tested (Fig. 1A). Part of the mechanism by which cisplatin may cause cytotoxicity is the generation of ROS [50]. On the other hand, ovarian cancer cells have been shown to have very robust ROS sequestering capacity [7]. Thus we next determined the role of ROS as a contributing factor in cisplatin cytotoxicity, which would implicate the involvement of antioxidant pathway. We repeated the cisplatin treatments but this time included the ROS neutralising agent, N-Acetyl Cysteine (NAC) as well. We found that co-treatment with NAC greatly reduced cisplatin cytotoxicity in cell dependent manner demonstrating the involvement of ROS in such cytotoxicity. The cytoprotective action of NAC was more pronounced in PEO1 cell line than PEO4 (Fig. 1B).

We next argued that ROS involvement in cisplatin cytotoxicity might lead to engagement of the NRF2 mediated antioxidant response pathway. We found that cisplatin treatment induced total NRF2 levels in both cell lines, albeit, to different extents. PEO1 cells, which exhibited greater cytotoxicity, also induced higher levels of NRF2. In order to demonstrate whether the induction of total NRF2 also leads to activation of its antioxidant transcriptional program, we transfected the cells with ARE-containing PGL3 vector driving the expression of luciferase gene to report NRF2 mediated transcription. Consistent with previous study [7], we found higher basal NRF2 transcriptional activity in PEO1 cells as compared to PEO4. Cisplatin challenge caused significant induction in both cells lines, however, higher induction was seen in PEO1 (Fig. 2B). These initial findings demonstrated the involvement of ROS in cisplatin cytotoxicity leading

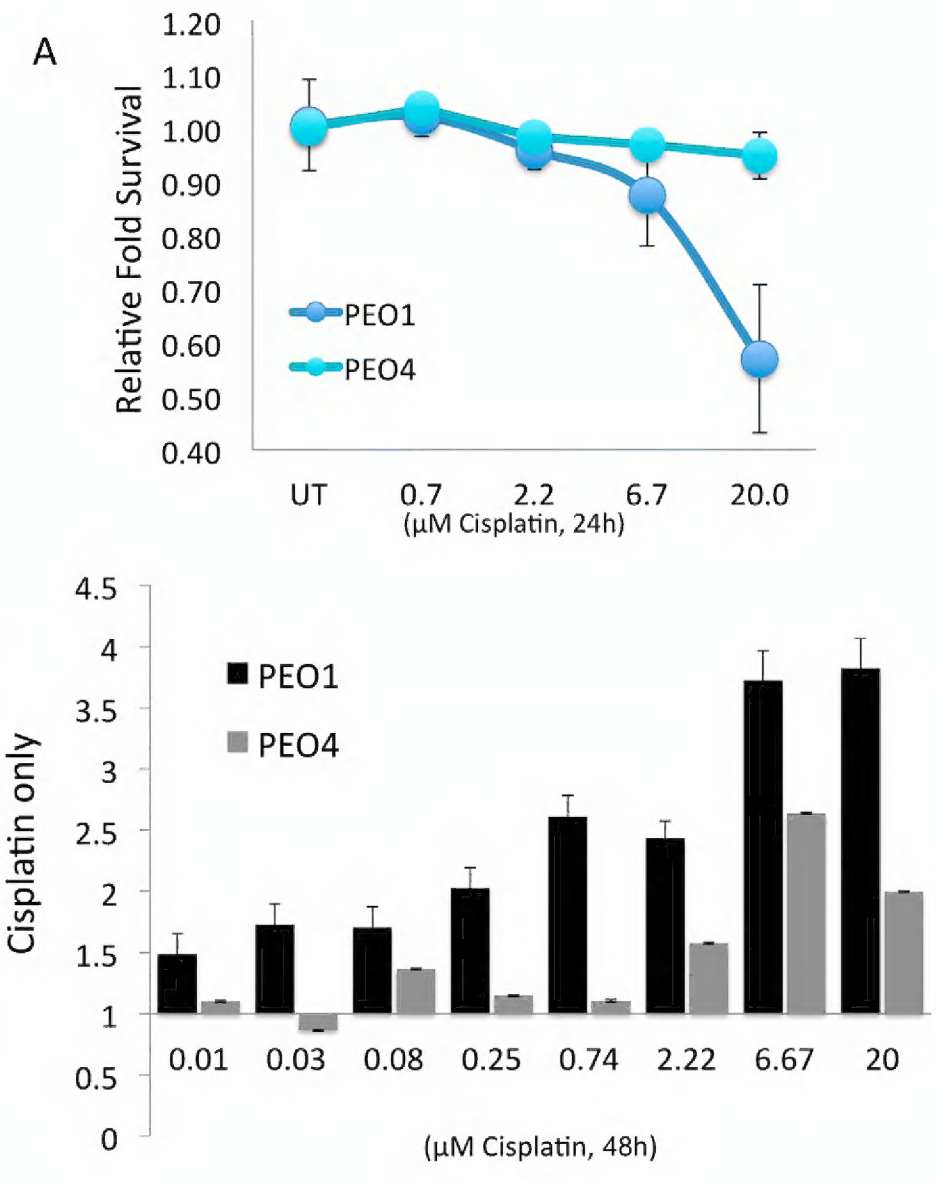

Figure 1. Cisplatin treatment causes different degree of cytotoxicity in PEO1 and PEO4 cell lines, which is partially relieved by N-Acetyl Cysteine (NAC) treatment. (A) Exponentially growing cells were seeded in 96 well plate in triplicates and allowed to attach for 18h. Following that, cells were either left untreated or treated with different concentrations of Cisplatin for further 24h. MTT reagent was added at the end of treatments and cells further incubated for 4h. The uptaken dye was released by adding 100μL of DMSO, shaking the plate for 15min and recording absorbance at 540nm using multiplate reader. Values are means of three replicates normalised to untreated (UT) controls expressed as 1. **(B)** Cells were seeded and subjected to different concentrations of Cisplatin treatment for 48h but this time also performing co-treatment with 20mM NAC to study the degree of its cytoprotection using MTT assay. Values are means with ± S.D of triplicates obtained by normalising to the corresponding values of cisplatin treatment alone at each concentration and expressed as 1.

to engagement of antioxidant response pathway also showing cell specific changes.

DNA Damage Response (DDR) pathway is intact in ovarian cancer cells and is induced following Cisplatin challenge

Cisplatin represents a central treatment modality for ovarian cancer and its main action is via DNA damage [46]. This could be via direct DNA binding and DNA adducts formation [51] or generation of ROS, which would further lead to DNA damage [50]. We next examined key proteins involved in DDR pathway to see which particular pathway is activated following cisplatin in our cell line model. Additionally, we also looked at phosphorylated NRF2, which is shown to represent activation of NRF2 [52]. Firstly, both at basal and induced states, PEO1 cell line showed higher levels of phospho NRF2 consistent with Fig. 2 (Fig. 3) illustrating a basally induced antioxidant pathway which is further activated following challenge. Secondly, while there were higher levels of basal and induced total and phospho P53 levels in PEO1 as well, PEO4 cell on the other hand exhibited higher levels of phospho ATM and phospho ATR. From Fig. 3, it is clear that at the concentration of cisplatin used here, ATM dependent DDR was activated while we could not see any phospho ATR induction. Hence, the phospho P53 induction seen could have resulted from ATM activity rather than ATR. Finally, we looked at γ-H2AX levels in these cells. γ-H2AX is a biomarker of DNA damage [35] and we used it to assess the degree of DNA damage sustained in the cell lines. Again, we found higher basal and induced levels of γ-H2AX in PEO1 cell line as compared to PEO4 possibly explained by higher cell death seen in Fig. 1.

Altogether, these results revealed cell specific degrees of cisplatin induced activation of ATM kinase

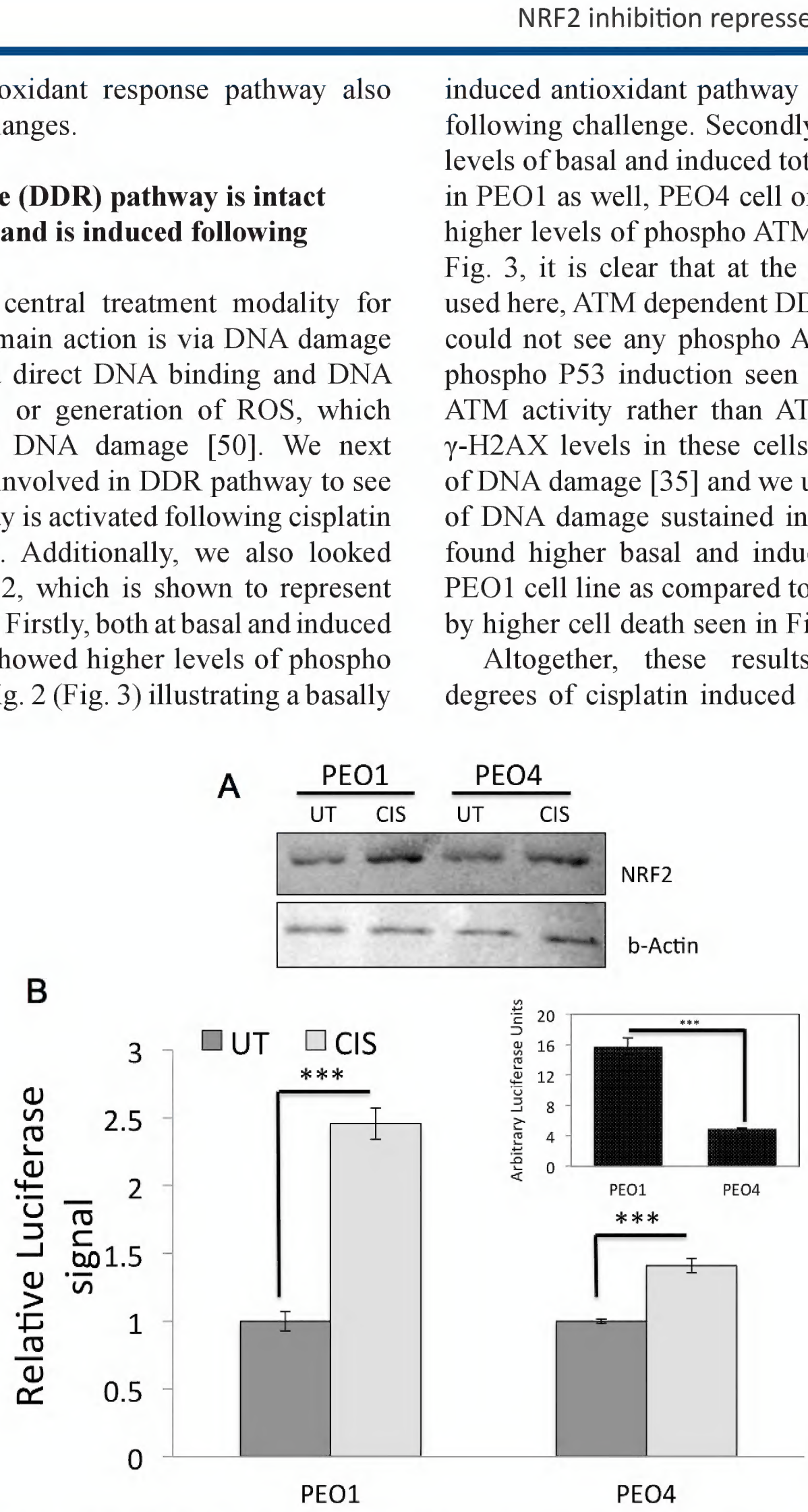

Figure 2. PEO1 exhibits higher basal and Cisplatin induced levels of NRF2 protein and transcriptional antioxidant response as compared to PEO4. (A) Immunoblotting analysis of constitutive and cisplatin induced levels of total NRF2 protein in PEO1 and PEO4 ovarian cancer cell lines shows higher basal and induced levels in PEO1. Exponentially growing cells were either left untreated (UT) or treated with 5μM Cisplatin for 5h. Following treatment, cells were harvested and protein lysates prepared and further processed for immunoblotting as mentioned in materials and methods and using anti NRF2 primary antibody (Table 1). **(B)** Transcriptional activity of NRF2 at basal and induced states in PEO1 and PEO4 demonstrates higher induction in PEO1. Exponentially growing PEO1 and PEO4 cells were transfected with either empty PGL3 basic vector or 1μg PGL3 basic vector with cloned NRF2 antioxidant response elements driving the expression of luciferase gene. Co-transfection with 0.2μg pRL-CMV plasmid was performed as an internal transfection control as described in the materials and methods. At 24h post-transfection, cells were either left untreated, or treated with 5μM Cisplatin for 24h. Following treatments, lysates were prepared and luciferase activity was measured using Dual luciferase reporter assay (Promega) in multiplate reader (MODULUS™, Promega). Inset shows basal transcriptional activity of NRF2 in the two cell lines. Data are the means with ± S.D of triplicates with statistical significance calculated by Student's *t* test according to the scale (* P <0.05, **P <0.01, ***P <0.001).

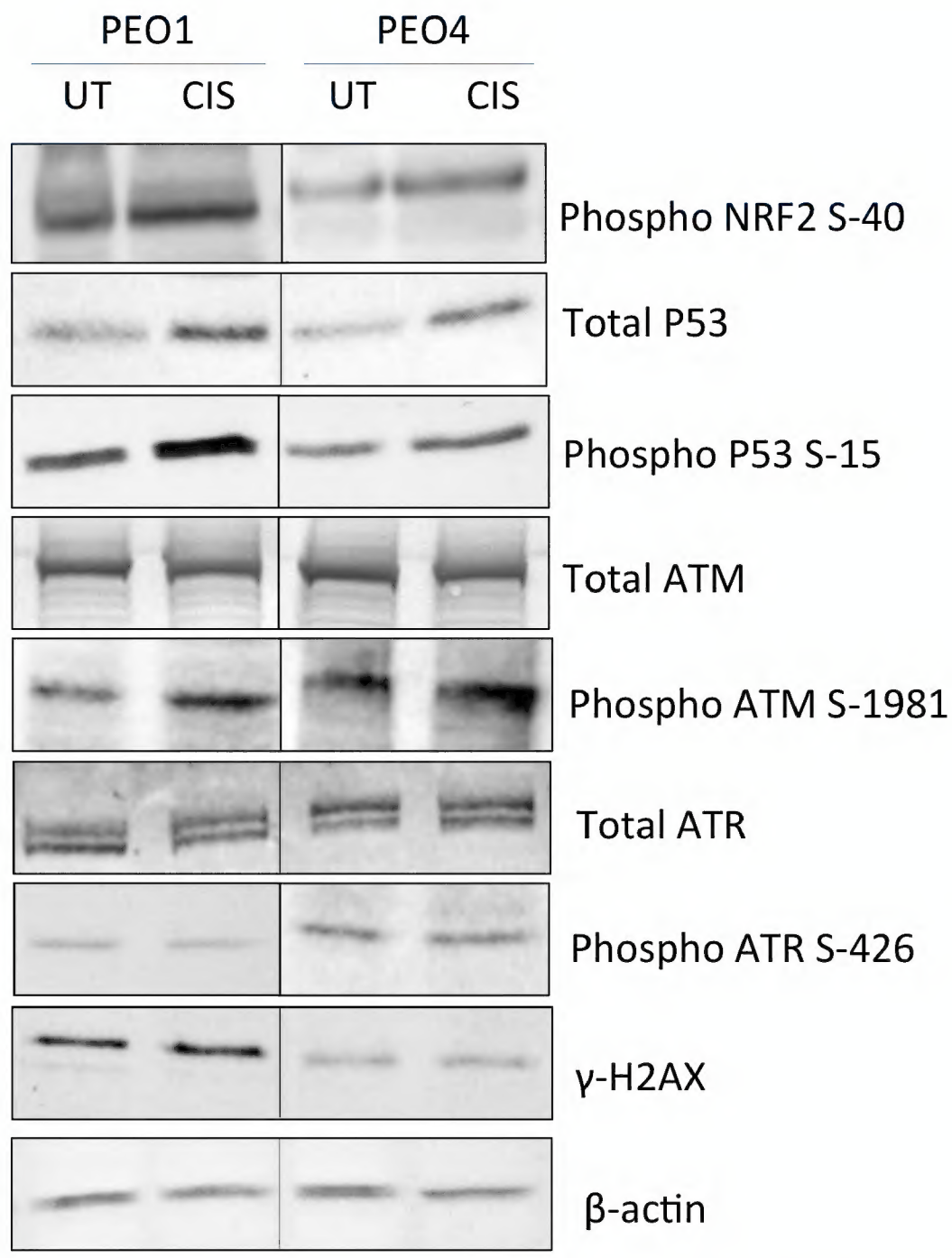

Figure 3. Cisplatin treatment induces ATM-dependent DNA damage response pathway in ovarian cancer cell lines. Immunoblotting analysis of DNA damage response (DDR) proteins in PEO1 and PEO4 ovarian cancer cell lines show cisplatin induced activation of DDR. Exponentially growing cells were either left untreated (UT) or treated with 5μM Cisplatin for 5h. Following treatments, cells were harvested and protein lysates prepared and further processed for immunoblotting as mentioned in materials and methods and using relevant antibodies (Table 1).

pathway as well as induction of phospho NRF2. This also suggests that both DDR and antioxidant response pathways are activated in these cancer cells.

Treatment with Retinoic acid (RA) inhibits antioxidant response pathway in ovarian cancer cells

In the previous section, we found that cisplatin treatment engaged both DDR and antioxidant response pathway. To further study this activation and determine whether such activation is interdependent and if there exists any co-regulatory mechanism, we either individually inhibited each pathway or co-inhibited them, repeated cisplatin treatment and examined the resulting protein expression, ROS levels and NRF2 transcriptional antioxidant response pathway. Previous studies have shown the inhibitory nature of RA on NRF2 [53]. We found that RA indeed repressed both total and phospho NRF2 protein levels (Fig. 4A). Additionally, RA further disrupted cisplatin-induced activation of these proteins, albeit more profoundly in PEO1.

In order to examine whether such cisplatin induced activation of NRF2 results in elevation of ROS, we performed an ROS quantitation assay on stable clones of MCF7 cells stably expressing 8 × *cis*-elements of antioxidant response to drive the expression of luciferase gene (AREc32, see methods). We found that 2.5μM RA significantly enhanced ROS levels at most of the cisplatin concentration assayed (Fig. 4B). Finally, using AREc32, we exposed cells to either RA or KU60019, a specific ATM kinase inhibitor (KU), or its combination and performed luciferase assay to measure the degree of NRF2 dependent transcription of antioxidant response genes. Firstly, we found that RA treatment significantly inhibited the antioxidant response in both absence and presence of cisplatin. Secondly, inhibition of ATM kinase alone did not significantly alter the antioxidant response as compared to UT control. Finally, the combination treatment using both RA and KU could not further inhibit antioxidant response as compared to RA alone (Fig. 4C), suggesting that while antioxidant response did

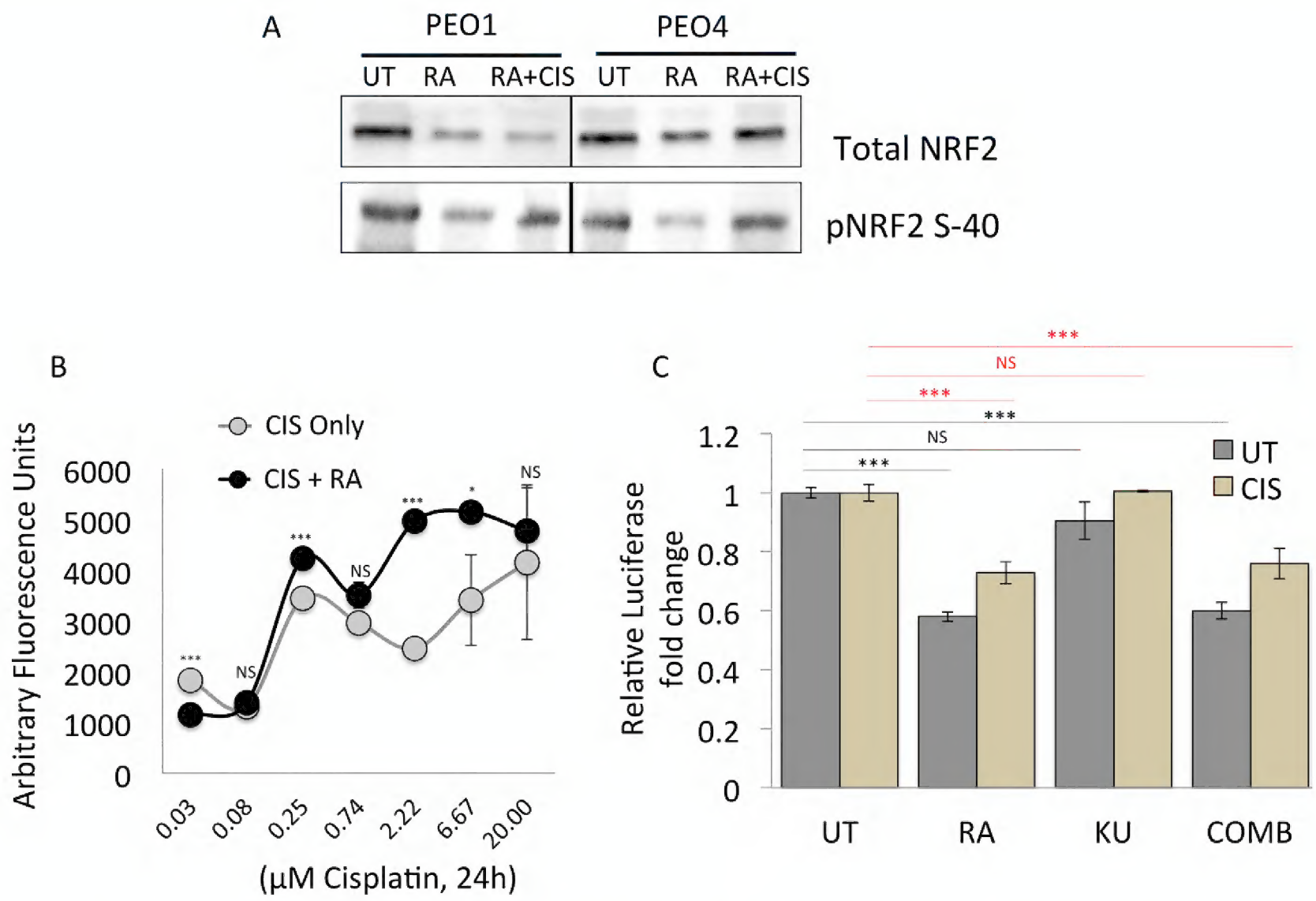

Figure 4. Retinoic acid (RA) treatment causes inhibition of NRF2-dependent antioxidant response in ovarian cancer cells. (A) RA causes repression of both constitutive and cisplatin induced protein levels of total and phospho NRF2. Exponentially growing cells were either left untreated (UT), treated with 2.5µM RA or 2.5µM and 5µM Cisplatin for 5h. Following treatments, cells were harvested and protein lysates prepared and further processed for immunoblotting as mentioned in materials and methods and using relevant antibodies (Table 1). **(B)** Cisplatin treatment causes dose dependent increase in reactive oxygen species (ROS), which is significantly further enhanced by co-treatment with RA. AREc32 cell line, stably expressing 8 x *Cis*-antioxidant response elements were seeded in triplicates in opaque flat bottom black walled 96-well plates for 18h and later treated with either different doses of cisplatin alone or in combination with retinoic assay for 24h. Following this, cells were assayed for total ROS by loading cells with DCFDA for 45min and measuring fluorescence using fluorescence multiplate reader (MODULUS™, Promega) with excitation and emission spectra of 485nm/535nm. The fluorescence reading recorded from each well was normalised to total cell abundance within the same wells as described in materials and methods **(C)** RA causes repression of NRF2 transcriptional antioxidant response. AREc32 cells were seeded in 96-well plates for 18h and exposed to either 2.5µM RA, 10µM KU60019 or their combination for 24h. Following this, cell lysates were prepared and processed for measuring luciferase activity by using Bright Glo™ Luciferase assay kit (promega) and recording data in multiplate reader (MODULUS™, Promega). The luminescence signal recorded from each well was normalised to the total protein content within same wells as described in material and methods. For **(B)** and **(C)** data are the means with ± S.D of triplicates with statistical significance calculated by Student's *t* test according to the scale (* P <0.05, **P <0.01, ***P <0.001).

not require ATM kinase activity, RA caused repression of phosphorylated and total NRF2, elevated ROS levels and inhibited antioxidant transcriptional program (Fig. 4).

RA induced inhibition of NRF2 causes repression of DDR pathway

Previous section demonstrated that while RA treatment disrupted the NRF2 dependent antioxidant response pathway, ATM inhibition was ineffective. Hence, next, we wanted to determine the consequences of NRF2 inhibition on DDR pathway instead, in order to investigate any co-regulation of the DDR pathway by NRF2. We found that RA treatment caused repression of both total ATM and ATR levels (Fig. 5) in both PEO1 and PEO4 cell lines. ATM and ATR are subject to autophosphorylation [54, 55]. Downregulation of these proteins hence suggested repression of their active phosphorylated forms too. Indeed, phospho ATM S1981 and phospho ATR S 426 were consistently found repressed upon RA treatment. As expected, their downstream substrate, P53 similarly exhibited reduced levels of phosphorylation following RA treatment. These interesting results demonstrated that inhibition of NRF2 protein caused inhibition of DDR pathway and downregulation of total ATM and ATR proteins. This further implicated that both antioxidant response and DDR pathways might be subjected to co-regulatory mechanisms.

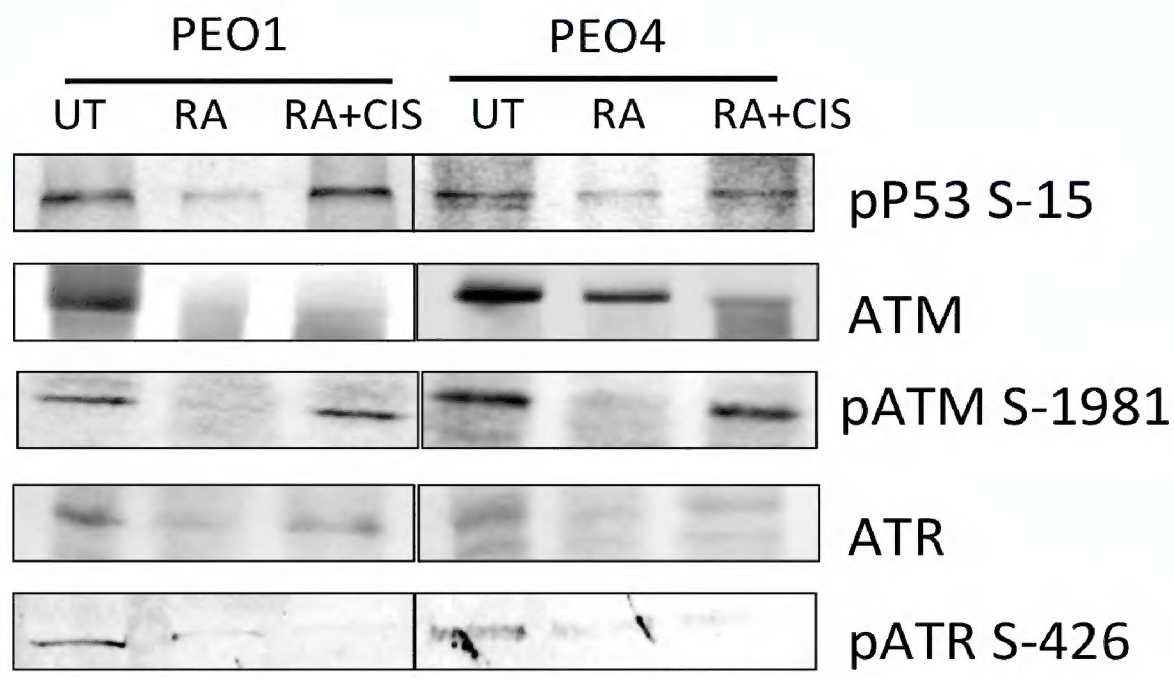

Figure 5. RA treatment causes repression of DDR proteins. Immunoblotting analysis of DDR proteins following RA treatment shows repression total and phosphorylated levels of ATM and ATR and phospho P53. Exponentially growing cells were either left untreated (UT) or treated with 2.5μM RA or 2.5μM RA + 5μM Cisplatin for 5h. Following treatment, cells were harvested and protein lysates prepared and further processed for immunoblotting as mentioned in materials and methods and using relevant primary antibodies (Table 1).

We further extended our investigation of the role of RA in DDR repression and performed whole cell ELISA on PEO4 cells previously exposed to different concentration of cisplatin (Fig. 6). This was done to determine whether RA can cause disruption of drug induced DDR activation and whether this disruption is independent of concentration of cisplatin used. Firstly, we found that treatment with RA alone significantly repressed total ATM levels in whole cell ELISA, consistent with previous immunoblotting result (Fig. 6A). While treatment with different doses of cisplatin caused dose dependent oscillation in total ATM levels, addition of RA with cisplatin caused repression as compared to each dose of cisplatin alone. Addition of KU to cisplatin on the other hand did not alter protein levels as compared to cisplatin only. Cisplatin treatment showed dose dependent induction of both total NRF2 (Fig. 6B) and phospho NRF2 (Fig. 6C). Consistent with Fig. 4, RA treatment alone downregulated total NRF2 levels, however in ELISA, such downregulation was not significant (Fig. 6B). Furthermore, while phospho NRF2 was inhibited by RA treatment, it was not significant (Fig. 6B). ATM kinase inhibition again failed to repress cisplatin induced pNRF2 activation at most of the cisplatin concentrations tested (Fig. 6C). This indicated that while repression of antioxidant pathway led to inhibition of DDR, inhibition of ATM on the other hand, did not alter phospho NRF2 induction following cisplatin challenge.

Upon finding the repression of DNA damage induced DDR by NRF2 inhibition, we furthered our study and investigated the kinetics of DDR pathway induction following time course treatment with cisplatin with or without NRF2 inhibition. We also did co-treatments with KU to examine how the DDR induction changes with such treatment in both PEO1 and PEO4 cell line (Fig. 7A) (Fig. 7B). In these experiments, we looked at phospho ATM, phospho Chk2, phospho P53 and γ-H2AX levels at different time points of treatment with 5μM cisplatin.

First of all, in both cell lines, treatment with RA alone reduced levels of phospho ATM, consistent with repression of total ATM seen in Fig. 6, phospho Chk2, phospho P53 and γ-H2AX (Fig. 7). However, as expected, there was more significant repression following KU treatment, which directly inhibits ATM kinase activity. Following cisplatin challenge, there was time dependent alteration in phospho ATM and induction in phospho P53 and γ-H2AX levels in both cell lines. While the inductions in the proteins were in oscillatory manner, such oscillations was not seen in phospho Chk2 levels in either of the cell lines. Strikingly, inhibition of NRF2 by co-treatment with RA repressed DDR protein induction at most of the time points tested. Finally, and as expected, inhibition of ATM kinase activity repressed phospho ATM levels at all the time points demonstrating its autophosphorylation mechanism. This caused repression of all the tested phosphorylated DDR substrates in both cell lines indicating the role of ATM kinase activity in their full induction.

These findings convincingly demonstrated that RA mediated NRF2 antioxidant pathway repression leads to an ineffective DDR pathway following cisplatin challenge both at different concentrations and for different time points of treatment.

Knockdown of NRF2 causes transcriptional repression of ATM and ATR kinases

In the current study we found that inhibition of NRF2 mediated antioxidant pathway led to repression of DDR signaling (Fig. 7) and downregulation of total ATM and

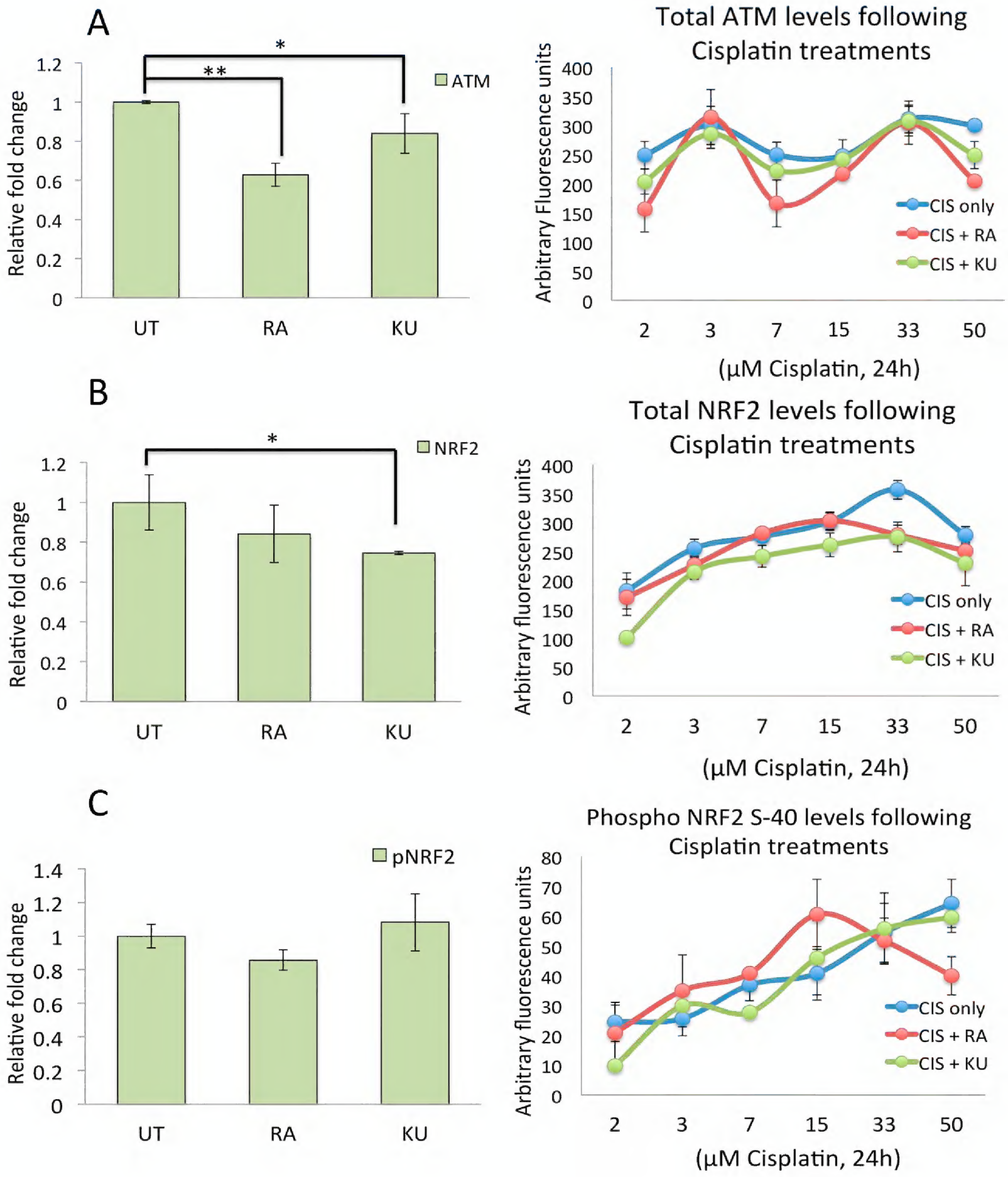

Figure 6. RA treatment alters dose dependent cisplatin-induced changes in total ATM, NRF2 and pNRF2 levels. **(A)** 2.5µM RA treatment causes significant protein repression of total ATM and influences cisplatin induced changes. Whole cell ELISA was carried out by seeding PEO1 cells in s opaque flat bottom black walled 96-well plates quadruplet for 18h. Following this, cells were either left untreated, treated with 2.5µM RA, or 10µM KU or different doses of cisplatin only, cisplatin with 2.5µM RA or cisplatin with 10µM KU. After a further 24h incubation, cells were processed for ELISA using primary ATM antibody followed by Alexa fluor 488-conjugated secondary antibody (Table 1) or primary NRF2 antibody and Alexa fluor 488-conjugated secondary antibody **(B)** or primary phospho NRF2 S-40 antibody and Alexa fluor 568-conjugated secondary antibody **(C)**. For (A), (B) and (C), the fluorescence signal was measured using fluorescent multiplate reader (MODULUS™, Promega) using relevant fluorescence channels. Data was normalised to total cell abundance from the same well as described in materials and methods. Values are means with ± S.D of quadruplet readings normalised to the untreated controls (UT) expressed as 1 in the left panels with statistical significance calculated by ONE WAY ANOVA followed by Tukey's post hoc test according to the scale (* $P < 0.05$, ** $P < 0.01$, *** $P < 0.001$).

ATR protein levels (Fig. 3). In order to understand the actual mechanism of ATM and ATR protein repression, we utilised 1kb upstream promoter regions of ATM and ATR genes cloned to drive luciferase gene expression for their transcriptional analysis using luciferase expression system (see materials and methods).

First of all, we saw significantly more expression of both ATM (Fig. 8A) and ATR (Fig. 8B) in PEO4 cell line as compared to PEO1. This was consistent with their total protein levels (Fig. 3). Interestingly, SiRNA

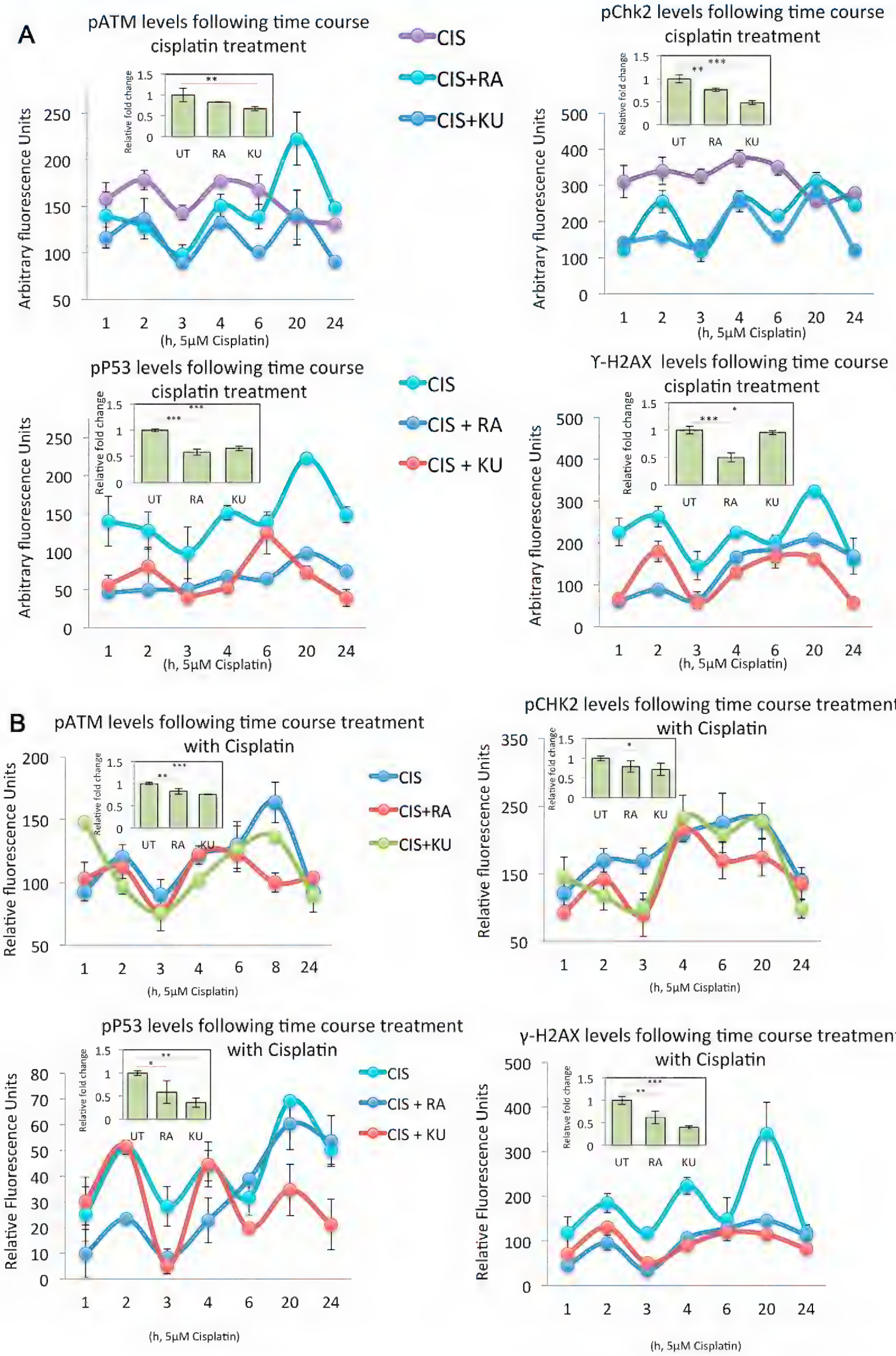

Figure 7. Time course treatment with Cisplatin shows time-dependent induction of DDR pathway, which is disrupted by co-treatment with RA. PEO1 cell line **(A)** and PEO4 cell line **(B)** exhibited RA dependent repression in DDR induction following treatment with 5µM Cisplatin for different time points as indicated. Cells were seeded in quadruplets in opaque flat bottom black walled 96-well plates and allowed to attach for 18h. Cell were either left untreated, or treated with either 2.5µM RA, 10µM KU for 24h or 5µM Cisplatin with either co-treatment of 2.5µM RA or 10µM KU for different time points as indicated. pATM S-1981 and pChk2-T68 were sequentially detected in same wells using Alexa fluor 488 and Alexa fluor 568 conjugated secondary antibodies respectively while pP53 and γ-H2AX were sequentially detected in same wells using Alexa fluor 488 and Alexa fluor 568 conjugated secondary antibodies respectively following relevant primary antibody incubations (Table 1). The fluorescence signal was measured using fluorescent multiplate reader (MODULUS™, Promega) using relevant fluorescence channels. Data was normalised to total cell abundance from the same well as described in materials and methods. Values are means with ± S.D of quadruplet readings. Insets show normalised data to the untreated controls (UT) expressed as 1 with statistical significance calculated by ONE WAY ANOVA followed by Tukey's post hoc test according to the scale (* P <0.05, **P <0.01, ***P <0.001).

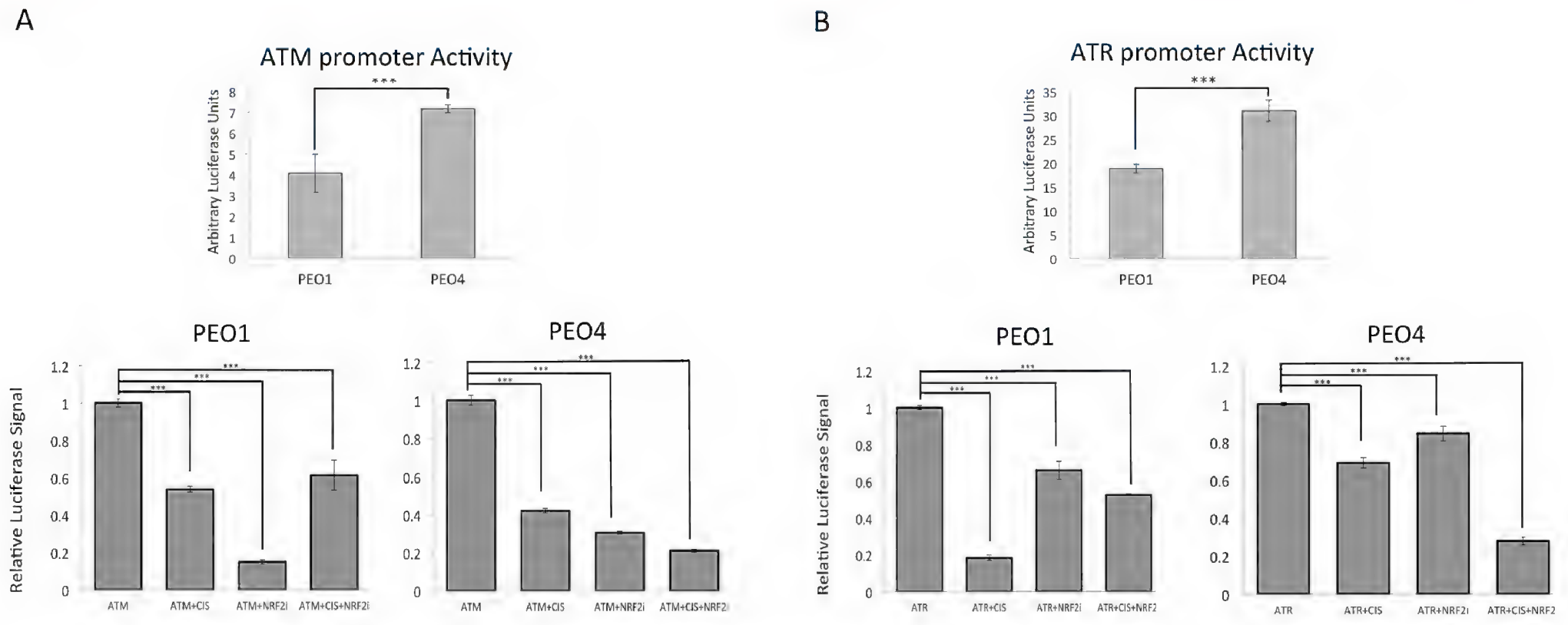

Figure 8. SiRNA-mediated knockdown of NRF2 results in downregulation of ATM and ATR transcription. (A) PEO4 cell line exhibits higher basal transcription of ATM while knockdown of NRF2 results in repression of ATM expression in both PEO1 and PEO4 cells. Exponentially growing PEO1 and PEO4 cells were seeded in 24 well plates and transfected with either empty PGL3 basic vector or 1µg PGL3 basic vector with cloned 1kb fragment of upstream ATM promoter region (prATM) driving the expression of luciferase gene. Co-transfection with 0.2µg pRL-CMV plasmid was performed as an internal transfection control as described in the materials and methods. Where required, co-transfection with SiRNA targeting NRF2 (NRF2i) was performed using 20pmol SiRNA as described in materials and methods. At 24 h post-transfection, cells were either left untreated, or treated with 5µM Cisplatin for 24h. Following treatments, lysates were prepared and luciferase activity was measured using Dual luciferase reporter assay (Promega) in multiplate reader (MODULUS™, Promega). **(B)** PEO4 cell line exhibits higher basal transcription of ATR while knockdown of NRF2 results in repression of ATM expression in both PEO1 and PEO4 cells. Same procedure performed as in (A) using 1kb fragment of upstream ATR promoter region (prATR) driving the expression of luciferase gene. In (A) and (B), data are the means with ± S.D of triplicates with statistical significance calculated by Student's *t* test (upper panels) or ONE WAY ANOVA (lower panels) Tukey's post hoc test according to the scale (* P <0.05, **P <0.01, ***P <0.001).

mediated knockdown of NRF2 resulted in repression of both ATM and ATR expression below basal levels and this repression was more pronounced in PEO1 cell line. Cisplatin treatment alone also resulted in repression of ATM and ATR transcription whereas combination of NRF2 knockdown and cisplatin together, in most cases, did not further repressed the transcriptional activities of ATM and ATR promoters.

These experiments explained the repression of total ATM and ATR protein levels following NRF2 inhibition seen in western blotting and suggested a transcriptional regulation of these kinases by NRF2. Since NRF2 is a transcription factor itself, it may directly bind to ATM and ATR promoter regions and repress their expression, or via indirect means, whereby, it might transcribe another protein, that in turn might regulate ATM and ATR transcription. To test these possibilities, more studies are needed to confirm the presence of NRF2 on ATM and ATR promoters.

Abnormal DDR signalling caused by NRF2 inhibition leads to enhanced cisplatin cytotoxicity in ovarian cancer cell lines

Transcriptional regulation of ATM and ATR by NRF2 and the fact that NRF2 inhibition led to transcriptional repression of these important DDR kinases provides an important strategy for sensitisation towards agents that otherwise activate ATM and ATR to induce repair pathways. To confirm this proposition, we exposed cells to different concentration of cisplatin but with co-treatments with either RA, or KU or their combination in PEO1 and PEO4 cell line (Fig. 9). First of all, we found that inhibition of ATM pathway with KU increased cisplatin cytotoxicity in both cell lines. However, a relatively greater sensitisation was seen in PEO4 cell line than PEO1 as compared to corresponding cisplatin treatments alone. Importantly, RA co-treatment greatly enhanced cisplatin cytotoxicity in both cell lines resulting in lower cell survival at all concentrations of cisplatin in comparison with cisplatin treatments alone or cisplatin and KU co-treatment. Interestingly, a combination of RA and KU treatment did not further enhance cisplatin cytotoxicity as compared to RA treatment alone (Fig. 9). These important results demonstrate that RA treatment, which was shown to repress NRF2 protein and disrupt the antioxidant response pathway, leads to downregulation of ATM and ATR, aberrant or insufficient DDR signalling, and greater cytotoxicity to cisplatin challenge even in those cells lines, which are otherwise resistant to cisplatin. As such, this strategy represents a novel avenue by which ovarian cancer cell resistance could be reversed.

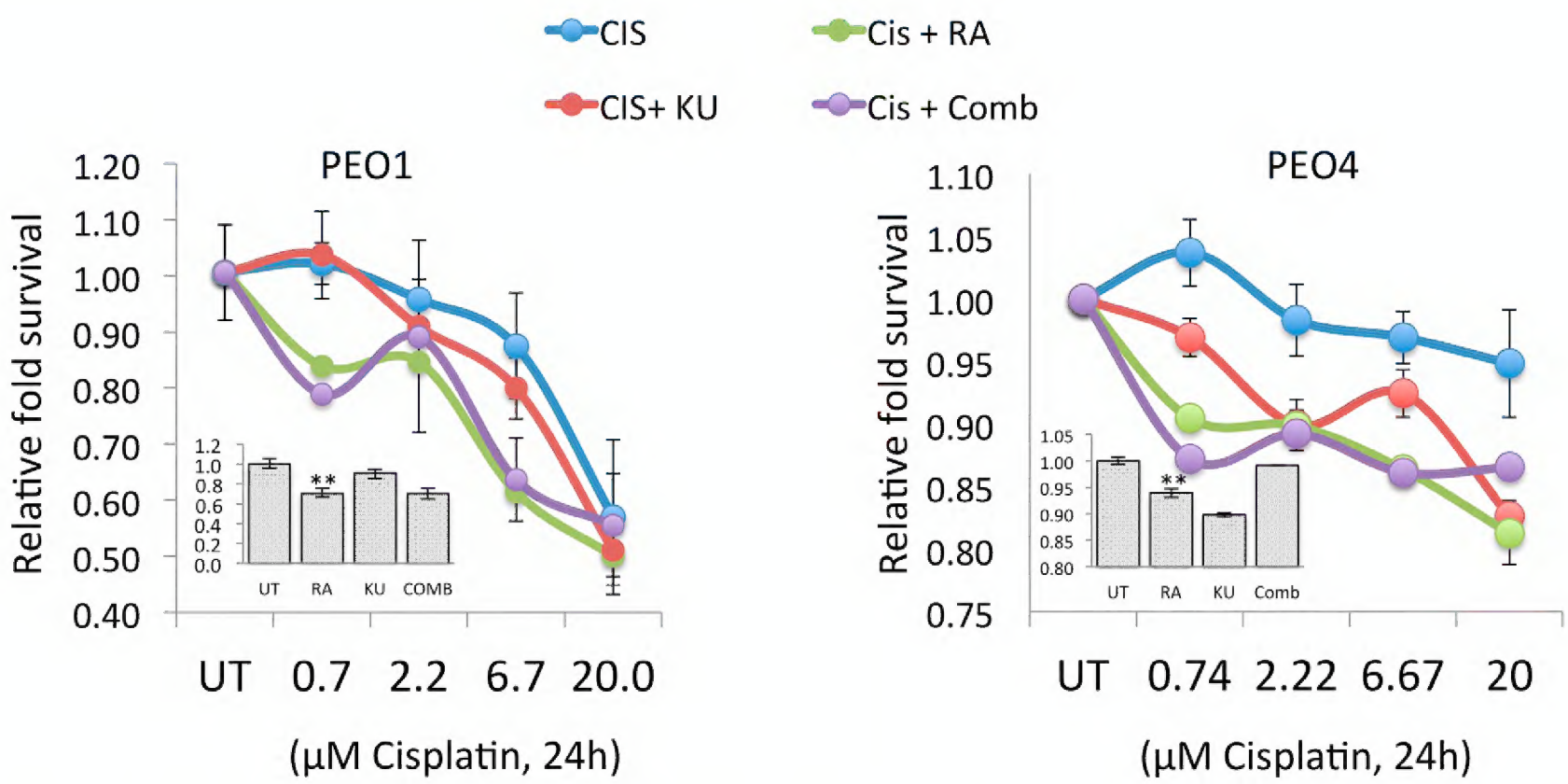

Figure 9. Inhibition of NRF2-dependent antioxidant response sensitises ovarian cancer cells to Cisplatin challenge. Exponentially growing cells were seeded in 96 well plate in triplicates and allowed to attach for 18h. Following that, cells were either treated with different concentrations of Cisplatin alone or cisplatin with either 2.5µM RA, 10µM KU or their combination for 24h. MTT reagent was added at the end of treatments and cells further incubated for 4h. The uptaken dye was released by incubation with 100µL of DMSO while shaking for 15min and recording absorbance at 540nm using multiplate reader (MODULUS™, Promega). Insets show fold change in survival relative to untreated cells (UT) following 2.5µM RA only, 10µM KU only, or their combination for 24h. Values are means with ± S.D of triplicates with statistical significance calculated by Student's *t* test according to the scale (* P <0.05, **P <0.01, ***P <0.001).

Discussion

Ovarian cancer cells have evolved robust inherent mechanism of cellular resistance towards both ROS and DNA damaging agents as demonstrated by a very effective antioxidant sensing and ROS neutralising mechanisms as well as a highly efficient DNA repair system [7, 41-44, 56]. ROS can trigger DNA damage that elicits ATM- and/or ATR-dependent signalling pathways to control cell cycle progression, apoptosis, and DNA repair. However, the manner by which ATM and ATR are transcriptionally controlled and then activated is not fully understood. Furthermore, while direct DNA damage induced ATM/ATR activation and DNA repair mechanism have got greater attention, the role of ROS in activating these kinases independent of DNA damage is less well clear. Although, ATM deficiency is associated with elevated cellular ROS, there is no evidence of a straight and a direct crosstalk between the cellular ATM/ATR-dependent responses of the DDR pathway with NRF2 of the AR pathways.

In this study we investigated the possibility of direct crosstalk between the NRF2 and the ATM/ATR pathways by analysing the direct functional interplay between AR and DDR pathways in a model of PEO1 and PEO4 ovarian cancer cell lines. These cell lines are more or less isogenic as they were isolated from a patient with ovarian adenocarcinoma at different stages of treatment. PEO1 cell line was isolated from malignant pleural effusions of the patient prior to treatment with cisplatin, 5-florouracil and chlorambucil, while PEO4 was isolated after the patient had developed resistance to these drugs [49].

Increased DNA damage repair has been implicated in the resistance of PEO4 to cisplatin [44, 58] and we have recently shown both PEO1 and PEO4 to have robust antioxidant sensing and sequestration mechanisms due to high level activated AR pathway [7]. The DDR and the AR pathways have both been linked with mechanisms of cisplatin resistance in ovarian cancer cells [41, 42, 44, 58, 59]. It is conceivable that these two pathways work concertedly to reduce the susceptibility of ovarian cancer cells to cisplatin. This is based on the premise that while ROS induced AR pathway will remove ROS, parallel activation of DDR pathway would still be required to repair the incurred DNA damage by ROS before its removal. To ascertain if these two pathways do crosstalk directly, the expression levels of protein of the AR and DDR pathways were assessed and compared with the transcriptional and posttranslational regulatory relationship between the proteins constituting these pathways.

Initial findings demonstrated the involvement of ROS and the engagement of AR pathway in cisplatin cytotoxicity in both PEO1 and PEO4 in a cell specific manner. We found that co-treatment of cells with NAC greatly reduced cisplatin cytotoxicity demonstrating the involvement of ROS in such cytotoxicity. The cytoprotective action of NAC was more pronounced in

PEO1 cell line than PEO4 (Fig. 1B), suggesting PEO1 to be either more oxidatively stressed than PEO4 or that PEO4 had greater inherent potential and propensity to overcome oxidative stress as compared to PEO1. This is supported by the observation that under both basal and cisplatin-induced states, PEO1 cell line showed higher levels of phospho NRF2 (Fig. 3) illustrating constitutively induced AR pathway, which was further activated following cisplatin challenge. Further, there were higher levels of basal and cisplatin-induced total and phospho P53 levels in PEO1 whereas, PEO4 cell exhibited higher levels of phospho ATM and phospho ATR. From Fig. 3, it is clear that at the concentration of cisplatin used, ATM dependent DDR was activated while we did not see any phospho ATR induction. Thus, the observed phospho P53 induction is likely and directly attributable to ATM activity rather than ATR, although ATR may be indirectly involved via contribution to the maintenance of phospho ATM [60]. Higher basal and cisplatin-induced levels of γ-H2AX were detected in PEO1 cell line as compared to PEO4 (Fig. 3), which is in consistence with the observed levels of phospho P53. This gives further support to our earlier assertion that PEO1 is either more oxidatively stressed than PEO4 or that PEO4 is more resistant to oxidative stress than PEO1. It is also indicative of the increased DNA repair capacity ascribed to PEO4 [44, 58]. Altogether, these results revealed cell specific degrees of cisplatin-induced activation of ATM kinase pathway as well as the induction of phospho NRF2, suggesting that both DDR and AR pathways are concurrently activated in these cancer cells.

Next, we used pharmacological inhibition to further delineate the concurrent activation of both DDR and AR pathways in these cancer cells. It appears that AR does not absolutely require ATM kinase activity for activation. Contrarily, RA caused repression of both phosphorylated and total ATM, inhibited the DDR pathway and elevated ROS levels (Fig. 4 and 5). These interestingly demonstrate that inhibition of NRF2 protein (Fig. 4) causes inhibition of DDR pathway and downregulation of total ATM and ATR proteins (Fig. 5), suggesting that both the AR and the DDR pathways might be subjected to co-regulatory mechanisms. Moreover, cisplatin treatment showed a dose dependent induction of both total NRF2 (Fig. 6B) and phospho NRF2 (Fig. 6C). Consistent with fig. 4, RA treatment alone significantly downregulated total and phospho NRF2 levels and ELISA further confirmed such downregulation (Fig. 6B). ATM kinase inhibition on the other hand, again failed to repress the cisplatin-induced phospho NRF2 activation at most of the cisplatin concentrations tested (Fig. 6C). Thus, while repression of AR pathway by RA led to inhibition of DDR, the inhibition of ATM again did not alter the induction of phospho NRF2 following cisplatin challenge.

Inhibitory action of RA on ATM and ATR activity also led to aberrant DDR induction following cisplatin challenge as demonstrated by reduced levels of DDR substrates phospho Chk2, phospho P53 and γ-H2AX (Fig. 7). However, as expected, there was more significant repression following KU treatment, which directly inhibits ATM kinase activity.

Interestingly, SiRNA mediated knockdown of NRF2 resulted in the repression of both ATM and ATR expression below constitutive levels and this repression was more pronounced in PEO1 cell line. Cisplatin treatment alone also resulted in the repression of ATM and ATR transcription (Fig. 8), which opens up the possibility of the existence of threshold levels and activation induced repression mechanisms [38]. Indeed combination of NRF2 SiRNA and cisplatin did not further repress the transcriptional activities of ATM and ATR promoters. These experiments thus explained the repression of total ATM and ATR protein levels and aberrant DDR following NRF2 inhibition seen in western blotting by suggesting transcriptional mechanism of regulation of these kinases by NRF2.

NRF2 is a transcription factor which may directly bind to ATM and ATR promoter regions and drive their expression. Bioinformatics analysis of our cloned ATM and ATR promoter regions suggested the presence of some putative AREs within, however more studies are needed to confirm the presence of NRF2 on ATM and ATR promoters. Another possibility is by indirect means, whereby, NRF2 might transcribe another protein that in turn regulates ATM and ATR transcription.

In conclusion, our current study provides a novel role of NRF in the transcriptional regulation of ATM and ATR. NRF2 inhibition led to transcriptional repression of these important DDR kinases and as such provides an important strategy for cellular sensitisation to overcome agents that otherwise activate ATM and ATR to induce DNA repair pathways. The repression of NRF2 protein and the disruption of the AR pathway leads to downregulation of ATM and ATR, aberrant or insufficient DDR signalling, and greater cytotoxicity to cisplatin challenge even in cisplatin resistant cells lines. As such, this represents a novel strategy to reverse and overcome ovarian cancer cell resistance to therapeutic agents. It has better our knowledge and understanding of cellular response to oxidative stress and a feasible novel avenue of treating other oxidative stress disorders, in addition to cancers.

Acknowledgements

The authors thank Professor Simon Langdon and Professor C Roland Wolf for providing the ovarian cancer and AREc32 cell lines, respectively. The authors acknowledge the Northwood Charitable Trust for financial support.

References

1. Jaiswal AK. Nrf2 signaling in coordinated activation of antioxidant gene expression. *Free Radic Biol Med. 2004*; **36(10):** 1199-207.
2. Niture SK, Khatri R, Jaiswal AK. Regulation of Nrf2-an update. *Free Radic Biol Med. 2013;* **66:**36-44.
3. Kimura M, Yamamoto T, Zhang J, Itoh K, Kyo M, Kamiya T, Aburatani H, Katsuoka F, Kurokawa H, Tanaka T, Motohashi H, Yamamoto M. Molecular basis distinguishing the DNA binding profile of Nrf2-Maf heterodimer from that of Maf homodimer. *J Biol Chem. 2007;* **282(46):** 33681-90.
4. Li W, Yu S, Liu T, Kim JH, Blank V, Li H, Kong AN. Heterodimerization with small Maf proteins enhances nuclear retention of Nrf2 via masking the NESzip motif. *Biochim Biophys Acta. 2008;* **1783(10):**1847-56.
5. Kaspar JW, Niture SK, Jaiswal AK. Nrf2:INrf2 (Keap1) signaling in oxidative stress. *Free Radic Biol Med. 2009;* **47(9):**1304-9.
6. Kobayashi M, Yamamoto M. Molecular mechanisms activating the Nrf2-Keap1 pathway of antioxidant gene regulation. *Antioxid Redox Signal. 2005;* **7(3-4)**: 385-94.
7. Khalil HS, Goltsov A, Langdon SP, Harrison DJ, Bown J, Deeni Y. Quantitative analysis of NRF2 pathway reveals key elements of the regulatory circuits underlying antioxidant response and proliferation of ovarian cancer cells. *J Biotechnol. 2015;* **202:** 12-30.
8. Hayes JD, McMahon M. NRF2 and KEAP1 mutations: permanent activation of an adaptive response in cancer. *Trends Biochem Sci. 2009;* **34(4):**176-88.
9. Shibata T, Ohta T, Tong KI, Kokubu A, Odogawa R, Tsuta K, Asamura H, Yamamoto M, Hirohashi S. Cancer related mutations in NRF2 impair its recognition by Keap1-Cul3 E3 ligase and promote malignancy. *Proc Natl Acad Sci U S A 2008;* **105(36):** 13568-73.
10. Ohta T, Iijima K, Miyamoto M, Nakahara I, Tanaka H, Ohtsuji M, Suzuki T, Kobayashi A, Yokota J, Sakiyama T, Shibata T, Yamamoto M, Hirohashi S. Loss of Keap1 function activates Nrf2 and provides advantages for lung cancer cell growth. *Cancer Res. 2008;* **68(5):** 1303-9.
11. Satoh T, Harada N, Hosoya T, Tohyama K, Yamamoto M, Itoh K. Keap1/Nrf2 system regulates neuronal survival as revealed through study of keap1 gene-knockout mice. *Biochem Biophys Res Commun. 2009;* **380(2):** 298-302.
12. Wakabayashi N, Itoh K, Wakabayashi J, Motohashi H, Noda S, Takahashi S, Imakado S, Kotsuji T, Otsuka F, Roop DR, Harada T, Engel JD, Yamamoto M. Keap1-null mutation leads to postnatal lethality due to constitutive Nrf2 activation. *Nat Genet*. 2003; **35(3):** 238-45.
13. Homma S, Ishii Y, Morishima Y, Yamadori T, Matsuno Y, Haraguchi N, Kikuchi N, Satoh H, Sakamoto T, Hizawa N, Itoh K, Yamamoto M. Nrf2 enhances cell proliferation and resistance to anticancer drugs in human lung cancer. *Clin Cancer Res. 2009;* **15(10):** 3423-32.
14. Hu Y, Rosen DG, Zhou Y, Feng L, Yang G, Liu J, Huang P. Mitochondrial manganese-superoxide dismutase expression in ovarian cancer: role in cell proliferation and response to oxidative stress. *J Biol Chem. 2005;* **280(47):** 39485-92.
15. Lister A, Nedjadi T, Kitteringham NR, Campbell F, Costello E, Lloyd B, Copple IM, Williams S, Owen A, Neoptolemos JP, Goldring CE, Park BK. Nrf2 is overexpressed in pancreatic cancer: implications for cell proliferation and therapy. *Mol Cancer. 2011;* **10:**37.
16. Reddy NM, Kleeberger SR, Yamamoto M, Kensler TW, Scollick C, Biswal S, Reddy SP. Genetic dissection of the Nrf2-dependent redox signaling-regulated transcriptional programs of cell proliferation and cytoprotection. *Physiol Genomics. 2007;* **32(1)**:74-81.
17. Ruiz-Ginés JA, López-Ongil S, González-Rubio M, González-Santiago L, Rodríguez-Puyol M, Rodríguez-Puyol D. Reactive oxygen species induce proliferation of bovine aortic endothelial cells. *J Cardiovasc Pharmacol. 2000;* **35(1):** 109-13.
18. Oluwaseun OA, Hilal S. Khalil. War without weapons – constitution of healthy and pathological phenotypes associated with polymorphisms in genes involved in the maintenance of genome integrity. *Biotechnol. & Biotechnol. Equip. 2012* **26(4):** 3073-78.
19. Chakarov S, Petkova R, Russev GCh, Zhelev N. DNA damage and mutation. Types of DNA damage. *Biodiscovery 2014;* **11:** 1.
20. Chakarov S, Petkova R, Russev GCh, Zhelev N. DNA repair and carcinogenesis. *Biodiscovery 2014;* **12:** 1.
21. Chakarov S, Petkova R, Russev GCh, Zhelev N. DNA damage and the circadian clock. *Biodiscovery 2014*; **13:** 1.
22. Berdelle N, Nikolova T, Quiros S, Efferth T, Kaina B. Artesunate induces oxidative DNA damage, sustained DNA double-strand breaks, and the ATM/ATR damageresponse in cancer cells. *Mol Cancer Ther. 2011;* **10(12):** 2224-33.
23. Tummala H, Khalil HS, Zhelev N. Repair, abort, ignore? Strategies for dealing with UV damage. *Biotechnol. Biotechnol. Equip. 2011;* **25(3):** 2443-46.
24. Jang SH, Lim JW, Morio T, Kim H. Lycopene inhibits Helicobacter pylori-induced ATM/ATR-dependent DNA damage response in gastric epithelial AGS cells. *Free Radic Biol Med. 2012;* **52(3):** 607-15.
25. Chaudhary P, Sharma R, Sahu M, Vishwanatha JK, Awasthi S, Awasthi YC.4-Hydroxynonenal induces G2/M phase cell cycle arrest by activation of the ataxia telangiectasia mutated and Rad3-related protein (ATR)/checkpoint kinase 1 (Chk1) signalling pathway. *J Biol Chem. 2013;* **288(28):** 20532-46.
26. Katsube T, Mori M, Tsuji H, Shiomi T, Wang B, Liu Q, Nenoi M, Onoda M. Most hydrogen peroxide-induced histone H2AX phosphorylation is mediated by ATR and is not dependent onDNA double-strand breaks. *J Biochem. 2014;* **156(2):** 85-95.
27. Kubota S, Fukumoto Y, Ishibashi K, Soeda S, Kubota S, Yuki R, Nakayama Y, Aoyama K, Yamaguchi N, Yamaguchi N. Activation of the prereplication complex is blocked by mimosine through reactive oxygen species-activated ataxia telangiectasia mutated (ATM) protein without DNA damage. *J Biol Chem. 2014;* **289(9):** 5730-46.
28. Ciccia A, Elledge SJ. The DNA damage response: making it safe to play with knives. *Mol Cell. 2010;* 40(2): 179-204.
29. Štarha P, Trávníček Z, Dvořák Z, Radošová-Muchová T, Prachařová J, Vančo J, Kašpárková J. Potentiating Effect of UVA Irradiation on Anticancer Activity of Carboplatin Derivatives Involving 7-Azaindoles. *PLoS One. 2015;* **10(4):** e0123595.
30. Khalil HS, Tummala H, Oluwaseun, OA, Zhelev N. Novel insights of Ataxia Telangiectasia Mutated (ATM) regulation and its potential as a target for therapeutic intervention in cancer. *Curr. Opin. Biotechnol. 2011;* **22(S1):** 115.
31. Khalil HS, Tummala H, Zhelev N. Differences in the DDR enzymes activation kinetics between normal and cancer cells could be utilized to achieve targeted cellular sensitivity towards genotoxic agents. *Cancer Research 2012;* **72:** 8.
32. Khalil HS, Tummala H, Chakarov S, Zhelev N. Targeting ATM pathway for therapeutic intervention in cancer. *Biodiscov*ery *2012;* **1:** 3.
33. Khalil HS, Tummala H, Zhelev N. ATM in focus: A damage sensor and cancer target. *Biodiscovery 2012*; **5:** 1.
34. Khalil HS, Chakarov S, Zhelev N. *ATM - a damage sensor and cancer target*. 2014, DSP, Dundee, Edinburgh, London
35. Khalil HS, Tummala H, Hupp TR, Zhelev N. Pharmacological

inhibition of ATM by KU55933 stimulates ATM transcription. *Exp Biol Med* (Maywood). *2012;* **237(6):** 622-34.
36. Khalil, HS, Tummala H, Zhelev N. Phosphorylated ATM at S-1981 (pATM) undergoes COPI mediated Golgi export upon DNA damage. *FEBS J. 2012;* **279(S1):** 146.
37. Khalil H.S., Tummala H., DeCaris L., Zhelev N. Pharmacological inhibition of ATM results in mitochondrial biogenesis in AMPK independent manner. *Cancer Res 2013*; **73(8):** 1697.
38. Idowu M, Khalil HS, Bown J, Zhelev. Reverse engineering of drug induced DNA damage response signalling pathway reveals dual outcomes of ATM kinase inhibition. *Biodiscovery 2013;* **9:** 4.
39. Bown JL, Idowu MA, Khalil HS, Goltsov A, Deeni Y, Zhelev N, Langdon SP, Harrison DJ. Process-based vs. data-driven modelling of cancer cell behavior. *J Biotechnol 2014*; **185(S):** S13.
40. Bartkova J, Horejsí Z, Koed K, Krämer A, Tort F, Zieger K, Guldberg P, Sehested M, Nesland JM, Lukas C, Ørntoft T, Lukas J, Bartek J. DNA damage response as a candidate anti-cancer barrier in early human tumorigenesis. *Nature. 2005;* **434(7035):** 864-70.
41. Selvakumaran M, Pisarcik DA, Bao R, Yeung AT, Hamilton TC. Enhanced cisplatin cytotoxicity by disturbing the nucleotide excision repair pathway in ovarian cancer cell lines. *Cancer Res. 2003;* **63(6):** 1311-6.
42. Jiang T, Chen N, Zhao F, Wang XJ, Kong B, Zheng W, Zhang DD. High levels of Nrf2 determine chemoresistance in type II endometrial cancer. *Cancer Res. 2010;* **70(13):** 5486-96.
43. Konstantinopoulos PA, Spentzos D, Fountzilas E, Francoeur N, Sanisetty S, Grammatikos AP, Hecht JL, Cannistra SA. Keap1 mutations and Nrf2 pathway activation in epithelial ovarian cancer. *Cancer Res. 2011;* **71(15):** 5081-9.
44. Wang QE, Milum K, Han C, Huang YW, Wani G, Thomale J, Wani AA. Differential contributory roles of nucleotide excision and homologous recombination repair for enhancing cisplatin sensitivity in human ovarian cancer cells. *Mol Cancer. 2011;* **10:** 24.
45. Wang XJ, Hayes JD, Wolf CR. Generation of a stable antioxidant response element-driven reporter gene cell line and its use to show redox-dependent activation of nrf2 by cancer chemotherapeutic agents. *Cancer Res. 2006;* **66(22):** 10983-94.
46. Galluzzi L, Senovilla L, Vitale I, Michels J, Martins I, Kepp O, Castedo M, Kroemer G. Molecular mechanisms of cisplatin resistance. *Oncogene. 2012;* **31(15):** 1869-83.
47. Parker RJ, Eastman A, Bostick-Bruton F, Reed E. Acquired cisplatin resistance in human ovarian cancer cells is associated with enhanced repair of cisplatin-DNA lesions and reduced drug accumulation. *J Clin Invest. 199;* **87(3):** 772-7.
48. Godwin AK, Meister A, O'Dwyer PJ, Huang CS, Hamilton TC, Anderson ME. High resistance to cisplatin in human ovarian cancer cell lines is associated with marked increase of glutathione synthesis. *Proc Natl Acad Sci U S A. 1992;* **89(7):** 3070-4.
49. Stronach EA, Alfraidi A, Rama N, Datler C, Studd JB, Agarwal R, Guney TG, Gourley C, Hennessy BT, Mills GB, Mai A, Brown R, Dina R, Gabra H. HDAC4-regulated STAT1 activation mediates platinum resistance in ovarian cancer. *Cancer Res. 2011;* **71(13):** 4412-22.
50. Marullo R, Werner E, Degtyareva N, Moore B, Altavilla G, Ramalingam SS, Doetsch PW. Cisplatin induces a mitochondrial-ROS response that contributes to cytotoxicity depending on mitochondrial redox status and bioenergetic functions. *PLoS One. 2013;* **8(11):** e81162.
51. Fichtinger-Schepman AM, van der Veer JL, den Hartog JH, Lohman PH, Reedijk J. Adducts of the antitumor drug cis-diamminedichloroplatinum(II) with DNA: formation, identification, and quantitation. *Biochemistry. 1985;* **24(3):** 707-13.
52. Pi J, Bai Y, Reece JM, Williams J, Liu D, Freeman ML, Fahl WE, Shugar D, Liu J, Qu W, Collins S, Waalkes MP. Molecular mechanism of human Nrf2 activation and degradation: role of sequential phosphorylation by protein kinase CK2. *Free Radic Biol Med. 2007;* **42(12):** 1797-806.
53. Wang XJ, Hayes JD, Henderson CJ, Wolf CR. Identification of retinoic acid as an inhibitor of transcription factor Nrf2 through activation of retinoic acid receptor alpha. *Proc Natl Acad Sci U S A. 2007;* **104(49):** 19589-94.
54. So S, Davis AJ, Chen DJ. Autophosphorylation at serine 1981 stabilizes ATM at DNA damage sites. *J Cell Biol*. 2009; 187(7): 977-90. Erratum in: *J Cell Biol. 2010;* **188(3):** 443.
55. Liu S, Shiotani B, Lahiri M, Maréchal A, Tse A, Leung CC, Glover JN, Yang XH, Zou L. ATR autophosphorylation as a molecular switch for checkpoint activation. *Mol Cell. 2011;* **43(2):** 192-202.
56. Deeni Y, Khalil HS, Goltsov A, Langdon S, Harrison D, Bown J. Quantitative analysis of proliferation behaviour of ovarian cancer cells with the dynamics of reactive oxygen species production and sequestration. *J. Biotech. 2014;* **185***: S1-S126.*
57. Langdon SP, Lawrie SS, Hay FG, Hawkes MM, McDonald A, Hayward IP, Schol DJ, Hilgers J, Leonard RC, Smyth JF. Characterization and properties of nine human ovarian adenocarcinoma cell lines. *Cancer Res. 1988;* **48(21):** 6166-72.
58. Sakai W, Swisher EM, Jacquemont C, Chandramohan KV, Couch FJ, Langdon SP, Wurz K, Higgins J, Villegas E, Taniguchi T. Functional restoration of BRCA2 protein by secondary BRCA2 mutations in BRCA2-mutated ovarian carcinoma. *Cancer Res. 2009;* **69(16):** 6381-6.
59. Joshi PM, Sutor SL, Huntoon CJ, Karnitz LM. Ovarian cancer-associated mutations disable catalytic activity of CDK12, a kinase that promotes homologous recombination repair and resistance to cisplatin and poly(ADP-ribose) polymerase inhibitors. *J Biol Chem. 2014;* **289(13):** 9247-53.
60. Stiff T, Walker SA, Cerosaletti K, Goodarzi AA, Petermann E, Concannon P, O'Driscoll M, Jeggo PA. ATR-dependent phosphorylation and activation of ATM in response to UV treatment or replication fork stalling. *EMBO J. 2006;* **25(24):** 5775-82.